



CHORUS

This is the accepted manuscript made available via CHORUS. The article has been published as:

Glassy dynamics and equilibrium state on the honeycomb lattice: Role of surface diffusion and desorption on surface crowding

Shaghayegh Darjani, Joel Koplik, Vincent Pauchard, and Sanjoy Banerjee

Phys. Rev. E **103**, 022801 — Published 8 February 2021

DOI: [10.1103/PhysRevE.103.022801](https://doi.org/10.1103/PhysRevE.103.022801)

Glassy Dynamics and Equilibrium State on the Honeycomb Lattice: Role of Surface Diffusion and Desorption on Surface Crowding

Shaghayegh Darjani^{1,2}, Joel Koplik^{3,*}, Vincent Pauchard¹, and Sanjoy Banerjee^{1†}

¹*Energy Institute and Department of Chemical Engineering,
City College of New York, New York, NY 10031, USA.*

²*Benjamin Levich Institute and Department of Chemical Engineering,
City College of the City University of New York,
New York, New York 10031, USA.*

³*Benjamin Levich Institute and Department of Physics,
City College of New York, NY 10031, USA.*

(Dated: January 11, 2021)

The phase behavior and adsorption kinetics of hard-core particles on a honeycomb lattice are studied by means of random sequential adsorption with surface diffusion. We concentrate on reversible adsorption by introducing a desorption process into our previous model and varying the equilibrium rate constant as a control parameter. We find that an exact prediction of the temporal evolution of fractional surface coverage and the surface pressure dynamics of reversible adsorption can be achieved by use of the blocking function of a system with irreversible adsorption of highly mobile particles. For systems out of equilibrium we observe several features of glassy dynamics, such as slow relaxation dynamic, memory effect and aging. In particular, the analysis of our system in the limit of small desorption probability shows simple aging behavior with a power-law decay. A detailed discussion of Gibbs adsorption isotherm for non-equilibrium adsorption is given, which exhibits hysteresis between this system and its equilibrium counterpart.

I. Introduction

The phase behavior and dynamics of adsorption in two dimensional systems are key aspects of many current research areas such as phase transitions in amphiphilic monolayers [1], emulsion stability due to particle adsorption at the interface [2–4], particle self-assembly into clusters [5–8], chemisorption on metal surfaces [9, 10], and the melting at an interface [11, 12].

Understanding the approach to the equilibrium state and the kinetics of adsorption are of great interest, particularly in separation and filtration, where both desorption and adsorption are present. Models accounting for desorption have also been used in vibrated granular systems [13, 14], and in the adsorption of asphaltenes at toluene/water interfaces [15]. Further examples of the relevance of desorption occur in response to changes in experimental conditions, such as changing the pH of a solution, [16–18], rinsing with solvent or buffers [19, 20], variations in temperature [21], and the addition of surfactants [13].

The Langmuir model [22] has been widely used to describe the adsorption behavior of reversible systems [1, 23, 24]. However, the Langmuir model has limitations: it fails to provide satisfactory predictions for systems composed of interacting particles [25–27] and when the adsorbate is larger than the adsorption site [27, 28]. These deficiencies of the Langmuir model are addressed

by the random sequential adsorption (RSA) and lattice gas models, which describe the adsorption kinetics and equation of state (EOS) of a monolayer, respectively. **It is worth noting that if the adsorption does not follow the Langmuir model, the adsorption properties and EOS become sensitive to the underlying lattice geometry such as square [29, 30], triangle [31, 32], and honeycomb lattice [33, 34].**

In the RSA model, molecules or particles which are larger than the adsorption sites are sequentially added at random to an initially empty surface, with the restriction that overlaps are forbidden. As the coverage increases, the free area left for further adsorption decreases, not only because of the sites occupied by previously adsorbed molecules but also because vacancies can be too small to allow adsorption without overlap. In the absence of surface diffusion or desorption, the adsorption process rapidly slows down and coverage only asymptotically approaches the jamming limit, equivalent to random maximum packing. In this limit, the jamming coverage depends on the lattice structure, the size and shape of the adsorbed particles [33, 35]. However, several physical processes involve both adsorption and desorption, and here the system may stabilize in an equilibrium state below the maximum packing. In this situation, the RSA model with the addition of a desorption process has been used in the literature to study ion binding in Langmuir monolayer [16], the dynamics of ligand-substrate binding [36], the adsorption of fibrinogen molecules [37], and the decoration of microtubules with dimeric kinesin molecular motors [36]. All of these processes can be described *via* the simple RSA model at their early stage, while at higher coverage stage detachment and reattachment of

* jkoplik@ccny.cuny.edu

† banerjee@ccny.cuny.edu

species plays a major role. It has been observed experimentally that the relaxation time scale of adsorbed particles, due to their rearrangement on the surface, can be comparable to the deposition time scale [38]. Diffusional relaxation on the surface leads to a denser monolayer with a more ordered configuration where the steric hindrance effects of previously-adsorbed particles slows the process at the later stages [39].

The lattice gas model is a statistical mechanical approach to describe adsorbate configurations which, among other features, exhibits a phase transition at high surface coverage. This approach has been used to study phase transitions of photo-excited Rydberg gases [40], the self-assembly of isophthalic acid on graphite [41], the adsorption of selenium on a nickel surface [9], and the chemisorption of oxygen on palladium [42]. Although many versions of the lattice gas model have been studied in the literature, only the single case of a triangular lattice with first neighbor exclusion has an exact solution, given by Baxter [43]. For all other variants, a number of lattice gas methods have been developed over years based on various approximations: the matrix method of Kramer and Wannier [44–50], the density (or activity) series expansion method [44, 45, 51–55], the generalized Bethe method [56–58], Monte Carlo simulations [49, 59–63], the Rushbrooke and Scoins method [64], and fundamental measure theory [65]. Despite all of these efforts, the lattice gas model has not provided the adsorption kinetics of the system, and instead the main focus was the EOS and the nature of phase transitions.

In order to combine the advantages of the RSA and lattice gas models we previously developed an alternative method, the RSAD model, to derive the EOS of two-dimensional non-desorbing hard-core particles based on kinetic arguments and the Gibbs adsorption isotherm [on the triangular lattice](#) [66, 67]. One of the advantages of the RSAD model is its ability to locate the equilibrium state, ensuring that adequate thermalization had occurred and that finite size effects are negligible. In the RSAD model surface diffusion is introduced in parallel with adsorption so that vacancies large enough to adsorb further particles are both created and annihilated. When diffusion is sufficiently large, the size distribution of vacancies no longer depends on the history of adsorption (the positions where the adsorbates first arrived on the substrate) but only on the fractional surface coverage [68]. Note that in this model the potential energy is effectively infinite for particle overlap and zero otherwise, so that the system can therefore be considered as athermal [50, 62, 66]. Our results show that the RSAD model can be used as an equilibrium model where the EOS, the phase transition coverage, and the nature of this transition are all in excellent agreement with the only available model with an exact solution in the literature [43].

Our past work on the RSAD model focused on irreversible adsorption of equilibrium states, but in this paper we substantially extend our previous RSAD approach by incorporating desorption process and further explore

the dynamics far from equilibrium. An important motivation is the experimental observation that when the relaxation time scale is much smaller than the experimental time-window, a system may evolve out of equilibrium [2, 16, 69]. In the remainder of this section we review the theoretical basis for the method and discuss the numerical implementation in Section II. A detailed discussion of our findings for both equilibrium and non-equilibrium systems is given in Section III and we summarize the paper in Section IV.

II. Simulation details

In RSAD approach, for a two-dimensional lattice gas in equilibrium with a three-dimensional solution of adsorbate molecules, the equality of chemical potential throughout the system leads to:

$$d\Pi = kT \frac{\Theta}{A_a} d \ln C. \quad (1)$$

Here, Π is the surface pressure, T is temperature, k is Boltzmann constant, A_a represents the interfacial area covered by a single adsorbate molecule, Θ is the fractional surface coverage, and C is the concentration of the (three-dimensional) solution. Integrating the above equation gives:

$$\int_0^\Theta \frac{\Theta}{C} \frac{\partial C}{\partial \Theta} d\Theta = \frac{A_a}{kT} \Pi, \quad (2)$$

from which we see that knowledge of the adsorption isotherm, the relationship between $C(\Theta)$, bulk concentration, and fractional coverage, enables one to calculate the EOS $\Pi(\Theta)$.

The adsorption isotherm, in turn, can be obtained through kinetic arguments. At equilibrium the rates of adsorption and desorption of molecules are equal:

$$K_a C (1 - \beta(\Theta)) = K_d \Theta, \quad (3)$$

where, K_a and K_d are the adsorption and desorption rate constants, respectively, and $\beta(\Theta)$ is the “blocking function”, the fraction of the surface area, which is excluded from further adsorption by already adsorbed molecules. Solving for C and inserting the resultant expression into the integral version of the Gibbs adsorption isotherm yields:

$$\int_0^\Theta (1 - \beta(\Theta)) \frac{\partial}{\partial \Theta} \left[\frac{\Theta}{1 - \beta(\Theta)} \right] d\Theta = \frac{A_a}{kT} \Pi. \quad (4)$$

Thus, the blocking function is the only information needed to calculate the EOS, and we have shown previously [66, 67] that for lattice gases the blocking function can be precisely extracted from RSAD simulations.

From the definition of the adsorption rate, used above to define adsorption equilibrium, the blocking function can be extracted from the numerical simulations through the derivative of surface coverage with respect to the time:

$$\frac{\partial\Theta}{\partial t} = \frac{K_l}{1+K_l}(1-\beta(\Theta)) - \frac{\Theta}{1+K_l}, \quad (5)$$

where $t = nA_a/A$, n is the number of attempts, A is the total number of sites, and $K_l = K_a/K_d$. The blocking function can be further obtained from the rebuttal rate of adsorption attempts. In the absence of desorption ($K_l = \infty$), with highly mobile particles the system can reach the full coverage. For the system of non-desorbing particle in equilibrium, Eq. 5 reduces to:

$$\frac{\partial\Theta}{\partial t} = 1 - \beta(\Theta). \quad (6)$$

Blocking function in Eq. 6 is obtained from adsorption or desorption method described later in detail.

The adsorption of hard-core molecules with first neighbor exclusion on the honeycomb lattice involves the adsorption of molecules covering two adsorption sites (see Figure 1). Here, we employ two complementary methods as described in our previous works [66, 67]: an “*adsorption method*”, which begins from an empty lattice, and a “*desorption method*”, which begins with a full lattice and progressively decreases coverage. In the *adsorption*

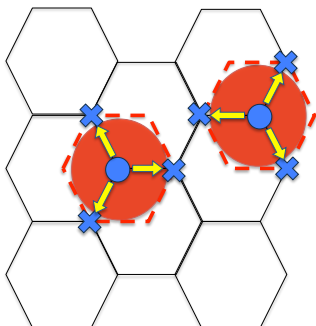


FIG. 1: Honeycomb lattice with first neighbor exclusion where each adsorbate covers 2 sites which is identified by red circles. The center of the adsorbate is represented by a blue circle, arrows indicate possible displacements of particles, and the blue crosses represent the sites where the center of other particles are not allowed to occupy.

method, molecules or particles are progressively added to an initially empty $d \times d$ lattice surface where a periodic boundary condition is used to ameliorate finite size effects. The only restriction is that overlap is not allowed; an assumption based physically on short-range electrostatic repulsion. For each adsorption attempt, a random position (x, y) is selected representing the center of mass of the particle. If the selected site and its neighbors are empty, adsorption is accepted, otherwise, it is rejected. Diffusion, the simultaneous movement of particles, is introduced sequentially with a predefined ratio D between

the number of diffusion attempt and the adsorption attempt: For $D = 3$ each adsorption is followed by 3 diffusion attempts, etc. For each diffusion attempt, a previously adsorbed particle and a direction for the displacement of the particle are selected randomly; yellow arrows in Figure 1 illustrate the possible directions. If moving the center of mass of the particle to the next node along this direction does not infringe the non-overlap condition, diffusion is accepted. Otherwise it is rejected. It is worth noting that in the RSAD model, when diffusion is fast enough, the surface layer is at internal equilibrium (even during transient adsorption) and the blocking function can be considered as a state function.

For the *desorption method* the lattice is initially full. In this method, two particles are randomly selected and removed. Then one adsorption attempt and D diffusion attempts are performed, until one particle is successfully deposited, following the same procedure as for the *adsorption method*. The choice of the sequence (2 desorption events followed by 1 adsorption) is arbitrary but answers the need at each time step to decrease coverage and add at least one particle to calculate the adsorption rate. Note that “*desorption method*” is another way to calculate the adsorption rate in a reverse order.

For both adsorption and desorption methods, the blocking function is extracted from the rebuttal rate of adsorption attempts. 500 independent runs are performed, and an ensemble average is used to reduce the noise arising from the numerical calculation of the derivative of the coverage. The blocking function is fitted with a polynomial function before using to generate the adsorption isotherm. The latter is inserted into the Gibbs adsorption isotherm equation to obtain the EOS.

In the current study, we have additionally incorporated desorption into the system aiming to validate our hypothesis that the correct evolution of fractional surface coverage and its equilibrium value, as well as blocking function can be faithfully predicted for systems with different values of K_l , provided we have the knowledge of the system with $K_l = \infty$. In this method, at each attempt, we randomly choose a site with a pre-defined value of K_l . The desorption attempts are carried out as follows: if a chosen site lies inside the adsorbed particle (inside the red circle illustrated in Figure 1), that particle is removed. Otherwise, we choose randomly one of the three neighboring sites and if that belongs to the center of mass of an adsorbate, we remove that particle. It is worth noting that in this case the desorption attempt imposes kinetic constraint as particle removal can be rejected whereas in the *desorption method* two particles are enforced to be removed. We performed these sets of simulations with and without surface diffusion. For a system with surface diffusion, after each attempt, D diffusion attempts are performed as described before. 1500 independent runs were performed to extract the success rate of adsorption attempts and to obtain the blocking function.

III. Results

The determination of phase behavior and, in particular, the nature of phase transitions in two-dimensional systems is often clouded by finite size effects and by access to the appropriate thermodynamic regime, which can bring uncertainty regarding phase behavior of the system; mainly the nature of phase transition [11, 67, 70, 71]. Accessing the thermodynamic regime and using sufficiently large system size to suppress errors due to finite size effects are initial steps toward studying the phase behavior of the system [11, 12, 67, 72]. One of the advantages of using the RSAD method is that we know how big our system should be to ensure that the results are both accurate and computationally inexpensive.

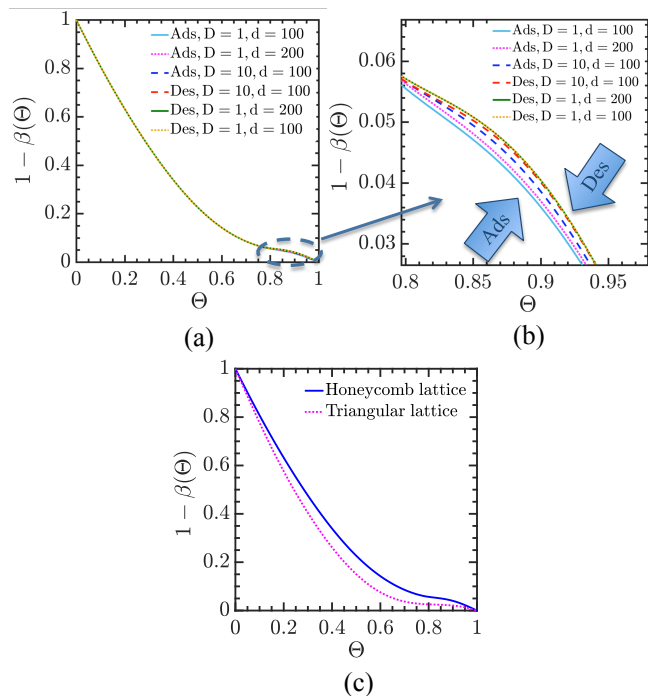


FIG. 2: (a) Effect of surface diffusion and lattice size on success rate of adsorption. Ads and Des refer to adsorption and desorption methods, respectively. (b) The inset magnifies the high-coverage region to better show the sensitivity of blocking function to surface diffusion and lattice size. (c) Comparison between the blocking function of the honeycomb and the triangular lattice [66].

The effect of surface diffusion and the system size are shown in Figure 2(a-b). Initially, when the system is dilute, all of the curves regardless of their methods, the magnitude of surface diffusion, or the system size coincide at the low surface coverage as presented in Figure 2(a). At high surface coverage, probability of success of adsorbing a new particle reduces drastically due to the caging effect. However, as the ordering of particles enhances, this caging effect diminishes to maximize the available surface for accepting the incoming particles. The system reaches the equilibrium state when curves obtained from

two methods (adsorption and desorption) overlap for the entire range of fractional surface coverage, which justifies the access to the thermodynamic regime. So, the results obtained from adsorption and desorption methods are expected to bracket the correct equilibrium EOS.

To assess the role of lattice geometry, we further compared the blocking function of hard-core particles with first neighbor exclusion on a honeycomb lattice with the ones on a triangular lattice [66] in Figure 2(c). Owing to extra lattice spacing between adjacent sites in the honeycomb lattice, lower blocking function is obtained over adsorption of particles compared to the triangular lattice.

EOS and phase transition of hard core molecules with the first neighbor exclusion on a honeycomb lattice were studied with various statistical mechanical approaches [34, 47, 73–75]. Runnels et al. [47] used an Exact Finite Matrix method, based on a sequence of exact solutions for lattices of infinite length and increasing finite width. The results were that, far from the transition zone, convergence occurs rapidly; while in the transition region, thermodynamic properties such as density and pressure are only functions of lattice width, which can be extrapolated to infinite width, giving the second order transition at critical density and surface pressure of 0.845 ± 0.02 and 2.24 ± 0.1 , respectively. Debierre et al. [73] used phenomenological renormalization method to obtain second order transition at fractional surface coverage and surface pressure of 0.83 ± 0.01 and 2.20 ± 0.02 , respectively. Baxter [74] found the critical component of hard core particle on honeycomb lattice by using corner transfer matrix and obtained second order transition at surface coverage of 0.844. Poland [75], used high density and Pade approximation to obtain the second order phase transition at a surface coverage of 0.822, and surface pressure of 2.164 and 2.178 for low and high density series, respectively.

Although all of these methods share similarities regarding the second order nature of the phase transition, however, there is no consensus on the critical value of a surface coverage at the transition. Our results have been compared with the analytical calculation of Runnels et al. [47] for $d = 100$ and $D = 10$ in Figure 3(a-b). As illustrated in Figure 3(a), at low surface coverage there is no difference between the reported equations of state. However, in vicinity of the phase transition a slight difference is observed (see Figure 3(b)). Runnels' EOS follows the *adsorption method* at a lower and the *desorption method* at a higher limit of surface coverage of transition region. Eventually, all of the EOS coincide as they approach the maximum packing coverage.

Comparing the EOS of honeycomb lattice with the triangular lattice [66] in Figure 3(c) shows that initially both equations of state overlap at a low surface coverage. As the surface coverage increases, triangular lattice shows higher surface pressure in vicinity of phase transition. Close to the maximum packing, finding the vacant site becomes the only determinant factor, consequently all of the equation of states obey the Langmuir model and

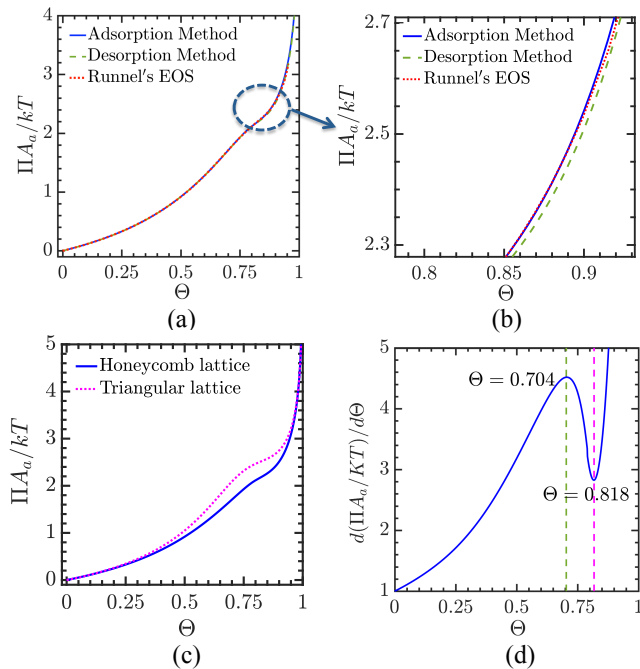


FIG. 3: (a) Comparison between our honeycomb EOS where $d = 100$ and $D = 10$ with Runnels et al. (Exact Finite Matrix method) [47] for hard core molecules on a honeycomb lattice. (b) The inset shows a magnified view of the EOS in the phase transition region. (c) Comparison between EOS of honeycomb and triangular lattice. A_a for honeycomb and triangular lattice are 2 and 3, respectively. (d) Analysis of phase transition region of honeycomb lattice based on derivative of surface pressure of desorption method with respect to the surface coverage ($d = 100$ and $D = 10$).

both lattice geometries display the same surface pressure.

The phase transition zone of honeycomb lattice is examined in more detail by taking the derivative of the surface pressure with respect to surface coverage, as displayed in Figure 3(d). A second order phase transition is obtained which is in agreement with others [34, 47, 73–75], where the critical exponents obtained by Debierre et al. [73] and others [34, 47] suggest that this system belongs to the 2-d Ising universality class. The onset of deviation from liquid regime starts at $\Theta = 0.704$ and system solidifies at $\Theta = 0.818$ and surface pressure of 2.169 ± 0.002 , where the adsorption and desorption methods set the upper and lower limit, respectively. Our results are in a good agreement with Poland [75]. Although, honeycomb and triangular lattice both display a second order phase transition, however, the triangular lattice deviates at the lower surface coverage $\Theta = 0.652$ from liquid regime and undergoes solidification at the higher surface coverage $\Theta = 0.827$, exhibiting a wider window of phase transition [66].

Systems with desorbing particles reach the equilibrium state below the maximum packing, as evidenced in many experimental studies [15]. We explored the role of desorption for a system in equilibrium (high surface diffusion), revealing that for different values of $K_{l,eq}$ same blocking

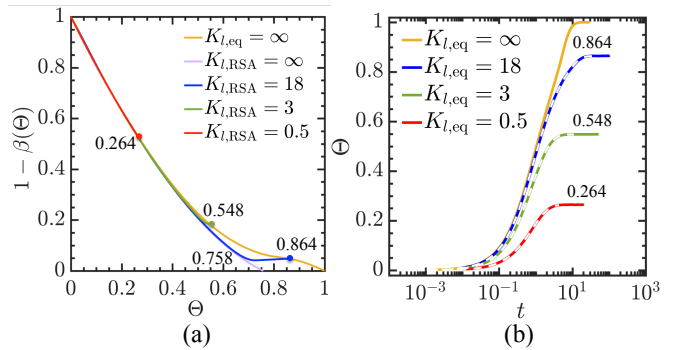


FIG. 4: (a) Blocking function for different $K_{l,RSA}$ where $d = 100$ and $D = 0$. Filled dots show the equilibrium values of surface coverage. (b) Time evolution of fractional surface coverage for different $K_{l,eq}$ where $d = 100$ and $D = 10$ in the presence of surface diffusion. White dashes lines are obtained from the prediction of RSAD model.

function is obtained as the one predicted by the Eq. 6 ($K_{l,eq} = \infty$ in Figure 4(a)) until the steady state value is achieved. The solid circles in Figure 4(a) denotes the steady state surface coverage for specified values of $K_{l,eq}$. Additionally, by plugging the blocking function obtained from Eq. 6 back into Eq. 5, we were able to obtain the time evolution of surface coverage for a given value of $K_{l,eq}$. These intriguing result are in an excellent agreement with the simulation results (see the white dashed lines in Figure 4(b)). Note that our simulations are performed on a homogeneous surface. However, surface heterogeneity can arise for example due to the variation in adsorption energy, nonuniform arrangement of the surface and etc. which could lead to the various structural ordering on the substrate [76, 77].

In the absence of surface diffusion and for $K_{l,RSA} = \infty$ (corresponding to a system with no desorption), system will reach the jamming state at the fractional surface coverage of 0.758 as illustrated in Figure 4(a). Jamming limit in RSA is strongly dependent on the initial configuration [13]. In the absence of surface diffusion, dynamics of adsorption, which can be described with RSA model pushes the system toward a locked or metastable configuration. Ordering is necessary to unlock this configuration, which is a slow process and can be mediated by detachment and reattachment of the particles [36]. Figure 4(a) shows that at the given fractional surface coverage, larger surface is available at equilibrium state compared to the RSA configuration [78].

For the RSA with desorption, adsorption process is dominant at the early stage and increasing the equilibrium rate constant results in the faster crowding of the surface. For small values of $K_{l,RSA}$ and when the surface is dilute, blocking function exactly overlaps on the equilibrium blocking function curve (see red curve in Figure 4(a)) [78–80]. However, for intermediate values of $K_{l,RSA}$ (e.g. green curve in Fig. 4(a)), system rapidly gets crowded while following the RSA curve and then slowly relaxes toward the equilibrium with the higher surface

coverage [14, 16] where insertion probability monotonically decreases by the increase of coverage [80].

For the system where the surface coverage surpasses the jamming coverage (see for example the blue curve for $K_{l,RSA} = 18$ in Figure 4(a)), the initial dominant adsorption process follow the RSA model and densifies the system in a very irregular fashion, making the deposition of a new particle very hard. At the late stage of the process the desorption plays a significant role and the success rate of adsorption shows an interesting trend in which after the initial abrupt decline, it increases very slowly with the increase of surface coverage, indicating a higher success rate of adsorption at a higher surface coverage. Note that the blocking function eventually reaches the steady state value identical to the equilibrium one. In the presence of desorption, the equilibrium rate constant (K_l) determines the equilibrium coverage while surface diffusion speeds up the process of reaching the equilibrium coverage without affecting the final value of coverage [14].

RSA with desorption shares qualitative similarities with many phenomenological properties of super-cooled liquid and glasses. For instance, as the $K_{l,RSA} \rightarrow \infty$, the system gets trapped in a metastable state and will not be able to relax toward the equilibrium. At high yet finite values of equilibrium rate constant, the early stage of this process suggests a mechanism similar to a quenched disorder which leads to the formation of supercooled liquid with frustrated structure. This analogy with supercooled liquid appearing at the early state, could be signaling the occurrence of aging phenomena at the late stage of the process. The aging phenomena is due to the strong memory effect originating from the high correlation with the initial configuration of the system where the relaxation evolves very slowly [85]. In order to quantify this out-of-equilibrium system and further validate our hypothesis regarding the aging process, we calculate two-time density-density correlation function [69, 82]:

$$C(t, t_w) = \frac{\langle \Theta(t)\Theta(t_w) \rangle - \langle \Theta(t) \rangle \langle \Theta(t_w) \rangle}{\langle \Theta(t_w)^2 \rangle - \langle \Theta(t_w) \rangle^2}, \quad (t \geq t_w). \quad (7)$$

Angular brackets indicate an ensemble average, and t_w is waiting time of sampling. Out of equilibrium, $C(t, t_w)$ depend on both t and t_w .

The aging properties of RSA with desorption for $K_{l,RSA} = 100$ is shown in Figure 5. The insertion probability of this system falls below the $K_{l,RSA} = 18$ in Figure 4(a) but follows the same trend. Figure 5(b) shows the disorder configuration of the system corresponding to a state that the insertion probability stops decaying. As the coverage slowly increases and the desorption process picks up, the degree of freedom in the system enhances and the decorrelation occurs due to the unlocking of the frustrated structure. As the the degree of ordering in the system enhances which is evidenced by the formation of clusters (see black clusters in Figure 5(c-d)), the $C(t, t_w)$

curves show an interesting trends where it follows the unique curve (see the black dotted lines in Figure 5(a)) which can be fitted with the following equation:

$$C(t, t_w) = (1 - q) \exp(-\alpha(t - t_w)) + q \left(\frac{t_w + t_s}{t + t_s} \right), \quad (8)$$

where q , α and t_s are fitting parameters. The constant q increases by increasing the $K_{l,RSA}$ and t_s is approximately equal to t_w . Figure 5(a) shows that correlation function follows two times sectors. Initially all of the correlation curves decay to a non-zero plateau value and follow the stationary exponential term in Eq. 8.

The exponential term in Eq. 8 is related to localized motion of particles within the cage which facilitates fast filling of the vacant sites and it obeys time-translation invariance independent of t_w [83, 84]. Then correlation curves decay from this plateau value to zero and follow the power law term (with exponent -1) in Eq. 8. The second decay depends on the waiting time and is called simple aging because it follows the power law. As the waiting time increases, the decorrelation takes longer, suggesting that cages are stiffer [85]. The second term implies the structural relaxation and appearance of cluster coarsening in the system where clusters merge by increase of t_w [83]. By passage of time, the clusters' coarsening result in the increase of insertion probability. Note that the equilibrium state (Figure 5(d)) is less blocked than the disorder configuration (Figure 5(b)). Eq. 8 suggests the weak-ergodicity breaking scenario where for $t > t_w$ correlation function decay as follow [84, 86]:

$$\lim_{t \rightarrow \infty} C(t, t_w) = 0, \quad (9)$$

$$\lim_{t_w \rightarrow \infty} C(t, t_w) = (1 - q) \exp(-\alpha(t - t_w)) + q, \quad (10)$$

$$\lim_{t_w \rightarrow \infty} \lim_{t - t_w \rightarrow \infty} C(t, t_w) = q, \quad (11)$$

q is Edwards-Anderson order parameter which can be defined from Eq. 11 [85]. In our system for $K_{l,RSA} = 100$, we find $q = 0.8257$.

We further address the influence of system's initial state on its dynamical response to a sudden change of K_l . The followings outline the series of simulations that were performed to obtain different initial states and once the system reached the target coverage ($\Theta = 0.758$) the simulations were stopped:

A) Starting from an empty lattice, the RSA with $K_{l2} = \infty$ were performed to achieve a glassy state with *much higher* blocking function compared to the equilibrium.

B) Starting from an empty lattice, the RSA were performed with a chosen value of $K_{l2} = 14$ that would result in steady state coverage above the target coverage of $\Theta = 0.758$ to achieve a system with a blocking function

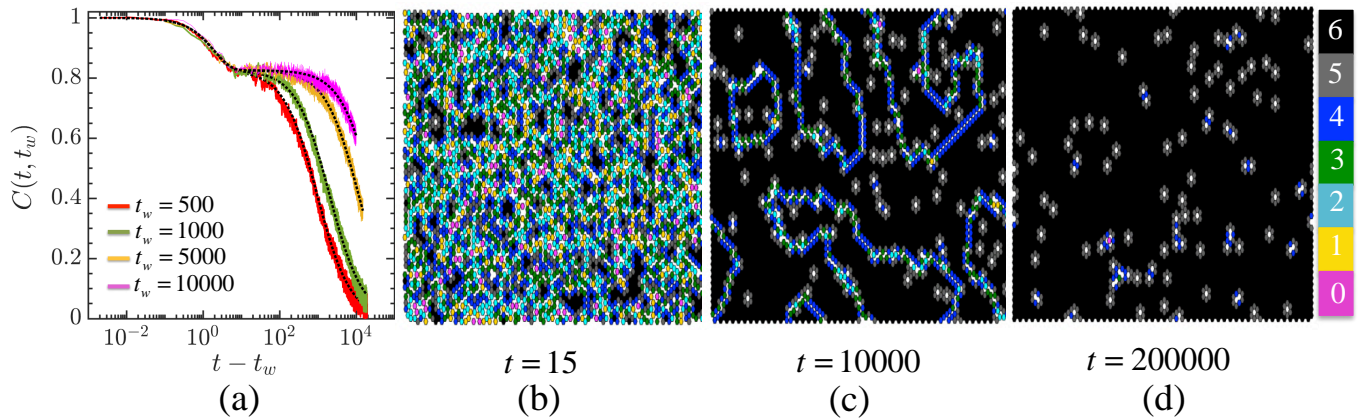


FIG. 5: (a) Two-time density-density correlation function at different t_w where $D = 0$, $d = 100$, $K_{l, RSA} = 100$. The black dotted lines are obtained from the Eq. 8. (b) The heatmap plot of the number of contacting neighboring sites for a system with $K_{l, RSA} = 100$ at different temporal surface coverages of (b) $\Theta = 0.7532$, (c) $\Theta = 0.9459$, (d) $\Theta = 0.979$. The color bar identifies the number of contacting neighbors.

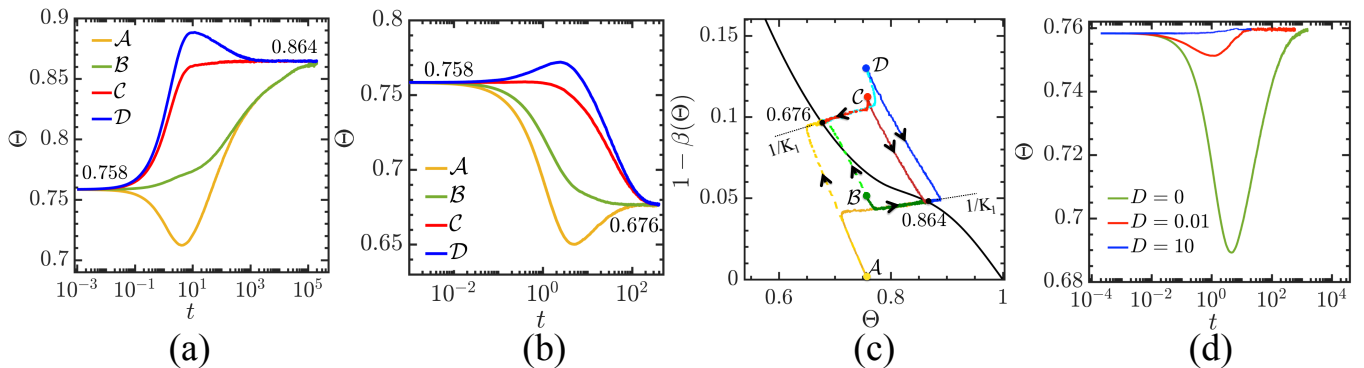


FIG. 6: Dynamical response of the system to abrupt change of K_{l2} to (a) $K_{l3} = 18$ and (b) $K_{l3} = 7$ from different initial states \mathcal{A} , \mathcal{B} , \mathcal{C} , and \mathcal{D} . (c) The insertion probability of adsorption for different initial states \mathcal{A} , \mathcal{B} , \mathcal{C} , and \mathcal{D} over abrupt change of K_{l2} to $K_{l3} = 18$ and $K_{l3} = 7$ corresponding to panels (a) and (b). (d) Dynamical response of the system with initial jammed configuration to the sudden change of K_l (from ∞ to 11.62) for different values of surface diffusion.

higher than the equilibrium state.

C) For a steady state system with high coverage, the value of $K_{l1} = 18$ were dropped to a low value $K_{l2} = 0.5$, engendering a system with a blocking function *much smaller* than the equilibrium state.

D) For a fully packed system, the value of $K_{l1} = \infty$ were dropped to $K_{l1} = 0$ leading to a system with a blocking function *much smaller* than the equilibrium system.

Once the systems reached the target coverage from different paths described above, the value of K_{l2} were changed to a new value $K_{l3} = 18$ (Figure 6(a)) and $K_{l3} = 7$ (Figure 6(b)) to study the dynamical response of the system to this stimuli.

For the glassy state \mathcal{A} (see Figure 6(a-b)), a valley appears in the coverage temporal evolution curve, where the depth of the valley depends on the value K_{l3} . For larger K_{l3} , the depth will be shallower. However, this valley will disappear for a critical small value of K_{l3} and the coverage will decrease monotonically to reach the steady state

value. The opposite behavior is observed for the system with \mathcal{D} initial state by the appearance of a peak in the coverage-time plot (Figure 6(a-b)). However, the appearance of this peak depends on the value of K_{l3} . For \mathcal{B} (\mathcal{C}) state over sudden change of K_{l2} to $K_{l3} = 18$, where the steady state coverage is higher than the initial state, surface coverage will smoothly (abruptly) increases to reach the steady state value. The opposite trend is observed for sudden change of K_{l2} to $K_{l3} = 7$. Figure 6(a) shows that the time evolution of surface coverage, regardless of their history, overlap after some relaxation time.

To gain better insight on dynamical response of the system to different initial state, we further analyze the insertion probability. Figure 6(c) displays an interesting result that there is a specific path (identified by black dashed lines in Figure 6(c)) related to each value of K_l . If the initial state is above (below) of this path, the adsorption (desorption) process is initially dominant until it crosses this path and then there is a tug-of-war competition between adsorption and desorption along this

path until the system reaches the steady state value. If the crossing occurs on the right (left) of the equilibrium line (black line in Figure 6(c)), the surface coverage decreases (increases) to reach the steady state. This path is encoded in the memory of the system and the system retains a strong memory of its K_l history where the slope of this path is nearly equal to the inverse of K_l .

Dynamical response of an initially jammed system to the sudden change of K_l (from ∞ to 11.62) and for different values of surface diffusion has been investigated as shown in Figure 6(d). The judicious choice of $K_l = 11.6$ serves to drive the system towards the steady state coverage equal to the jamming coverage (the initial state of the simulation). This abrupt change results in the initial increase of desorption rate and consequently enhances the insertion probability of adsorption. For fast enough surface diffusion, system immediately reaches the steady state configuration. However, in the absence of surface diffusion or at low values, a minima appears in the time evolution plot of surface coverage which roots in the relaxation of caging effect.

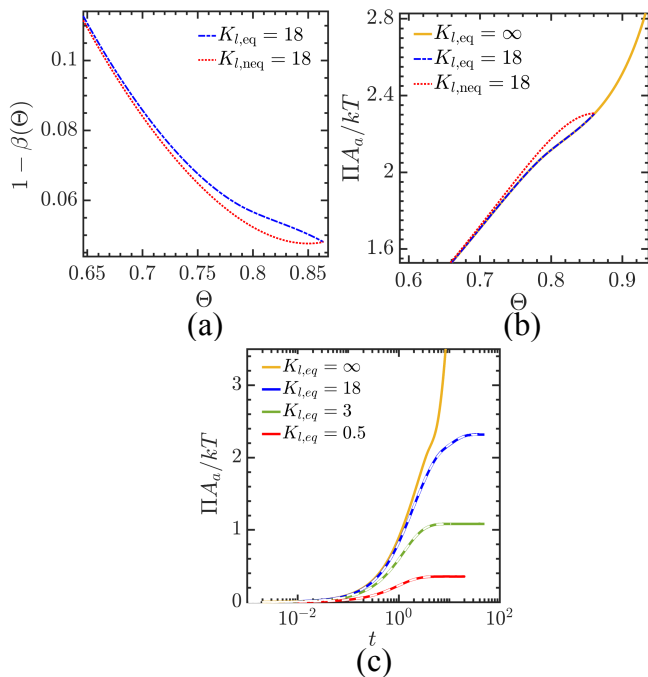


FIG. 7: (a) Success rate of adsorption for the equilibrium system $K_{l,eq} = 18$ and non-equilibrium system $K_{l,neq} = 18$ where $d = 100$. (b) Surface pressure versus surface coverage, (c) Time evolution of surface pressure for systems with various $K_{l,eq}$. White dashes lines are obtained from the prediction of RSAD model.

In hard-core system, internal energy is only a function of temperature and not a density [87]. Given hard-core interactions are athermal, all of the phase transitions are entropy driven, where ordered phase has a higher entropy than the disordered one [34, 87]. Consequently, we expect that the hysteresis between equilibrium system and its non-equilibrium counterpart comes from change

in configurational entropy [88]. Therefore, the blocking function and surface coverage would be the only required information to calculate the surface pressure. To corroborate our statement, we compared the surface pressure obtained from the blocking function for two systems with equal equilibrium rate constant of $K_l = 18$ but different surface diffusion $D = 0.01$ and $D = 10$, which are named $K_{l,neq} = 18$ and $K_{l,eq} = 18$, respectively (Figures 7(a), 7(b)). The blocking functions are the same for both systems at the steady state and also at low surface coverages (see Figure 7(a)). As such, we expect that at these two limits that the surface coverages overlap, the insertion of both equilibrium and non-equilibrium blocking functions (Figure 7(a)) into Eq. 4 yields to the same surface pressure. Figure 7(b) shows that the values of surface pressure at the equilibrium are exactly identical for both $K_{l,neq} = 18$ and $K_{l,eq} = 18$, which underscores the validity of our hypothesis. For systems in equilibrium, surface pressure is only a function of surface coverage as evidenced by the overlap of surface pressure curves for $K_{l,eq} = 18$ and $K_{l,eq} = \infty$. So, the knowledge of blocking function of a non-desorbing system at equilibrium ($K_{l,eq} = \infty$) would be sufficient to accurately obtain the surface pressure of the equilibrium systems with various $K_{l,eq}$. Figure 7(b) further displays that the surface pressure curve of non-equilibrium system is always higher than the equilibrium one as the system becoming gradually packed, which can explain the hysteresis observed in some experiments [2]. We also compare the time evolution of equilibrium surface pressure for systems with defined $K_{l,eq}$ and the results obtained from $K_{l,eq} = \infty$. This is accomplished by inserting the blocking function obtained from Eq. 6 into the Eqs. 4, 5 and integrating to obtain temporal evolution of surface pressures (identified by white dashed lines in Figure 7(c)) which shows an excellent agreement with the simulation results.

IV. Conclusion

In this paper we studied the phase behavior and adsorption kinetics of hard-core molecules with first neighbor exclusions on a honeycomb lattice, by incorporating a desorption process through a varying equilibrium rate constant in the RSAD model. Our analyses confirm earlier statistical mechanics results concerning the second-order nature of the phase transition [34, 47, 73–75]. We show that the system is in a disordered liquid regime below surface coverage of 0.704 and undergoes second-order transition at surface coverage of 0.818, which is in a good agreement with the work of Poland [75] who used high density and Pade approximation methods to obtain the EOS.

Comparing the results of hard-core particle on a honeycomb lattice with a triangular lattice [66] shows that the blocking function is sensitive to the lattice geometry. However, once the surface coverage and the blocking function are obtained from RSAD model, all other ther-

modynamic properties can be calculated from the same scheme explained in Section II irrespective of the lattice geometry. Higher surface pressure is obtained at intermediate surface coverage for the triangular lattice, while at low surface coverages and close to the maximum packing both lattice structures display the same surface pressure. Both lattice geometries show a second order phase transition, however, the triangular lattice undergoes a wider range of phase transition meaning that it deviates from the liquid regime at a lower surface coverage and solidifies at a higher surface coverage.

For the systems with desorption processes present, all of the results related to the temporal evolution of the blocking function, surface coverage, and surface pressure for various K_l can be derived from the blocking function of a system with $K_{l,eq} = \infty$. Taken together, RSAD model without desorption is able to accurately recover deposition dynamics results for systems with desorption.

In the absence of surface diffusion, the blocking function generated by RSA model including desorption shows three distinct regimes. Initially when the surface is dilute, the blocking function is identical to that in thermal equilibrium. At intermediate coverage, the blocking function initially follows the RSA model and then decreases monotonically to reach the equilibrium blocking coverage at the steady state. However, when the surface coverage surpasses the jamming coverage, the insertion probability of a new particle shows an interesting trend in which after the initial abrupt decline, it increases very slowly with the increase of surface coverage. At equilibrium and for a given value of the rate constant, the blocking function and surface coverage eventually recover the values for non-desorbing systems at equilibrium. Aging analysis of the last regime with small desorption probability through the two-time density-density correlation function shows two time sectors, where it initially follows the stationary regime and then decays as a power law. As the waiting time increases the decorrelation takes longer, which is an indication of a stiffer cage. As time passes, the structural relaxation and clustering of particles fa-

vor more densification which leads to a lower blocking function.

Analyses of the dynamical response of the system to an abrupt change of the rate constants K_l at different initial states reveals that there is a specific path toward equilibrium for each value of K_l , where the slope of this path is almost equal to $1/K_l$. This result also explains the appearance of a peak and a valley after a sudden change of K_l to a secondary value. For a system without surface diffusion, the system retains a strong memory of its history while the presence of surface diffusion results in the rapid decorrelation of memory effects.

Hard-core systems are entropy driven, and as such the blocking function and surface coverage would be the only information required to calculate the surface pressure. We show that the equilibrium surface pressure is insensitive to the values of surface diffusion and systems in that low and high values of surface diffusion result in identical surface pressure. Out of equilibrium and as the surface coverage is gradually increased, the system shows higher surface pressure than the equilibrium one, which could explain the hysteresis reported in some experimental observations.

Acknowledgments

This research was supported by the National Science Foundation under grant No. 1743794, PIRE: Investigation of Multi-Scale, Multi-Phase Phenomena in Complex Fluids for the Energy Industries.

Data Availability

The data that support the findings of this study are available from the corresponding author upon reasonable request.

-
- [1] V. Fainerman and D. Vollhardt, *J. Phys. Chem. B* **103**, 145 (1999).
 - [2] V. Pauchard, J. P. Rane, and S. Banerjee, *Langmuir* **30**, 12795 (2014).
 - [3] F. Liu, S. Darjani, N. Akhmetkhanova, C. Maldarelli, S. Banerjee, and V. Pauchard, *Langmuir* **33**, 1927 (2017).
 - [4] X. Hua, J. Frechette, and M. A. Bevan, *Soft matter* **14**, 3818 (2018).
 - [5] Z. Hou, K. Zhao, Y. Zong, and T. G. Mason, *Phys. Rev. Mater.* **3**, 015601 (2019).
 - [6] S. Fortuna, D. L. Cheung, and A. Troisi, *J. Phys. Chem. B* **114**, 1849 (2010).
 - [7] U. Weber, V. Burlakov, L. Perdigo, R. Fawcett, P. Beton, N. Champness, J. Jefferson, G. Briggs, and D. Petifor, *Phys. Rev. Lett.* **100**, 156101 (2008).
 - [8] V. Gorbunov, S. Akimenko, A. Myshlyavtsev, V. Fefelov, and M. Myshlyavtseva, *Adsorption* **19**, 571 (2013).
 - [9] P. Bak, P. Kleban, W. Unertl, J. Ochab, G. Akinci, N. Bartelt, and T. Einstein, *Phys. Rev. Lett.* **54**, 1539 (1985).
 - [10] D. E. Taylor, E. D. Williams, R. L. Park, N. Bartelt, and T. Einstein, *Phys. Rev. B* **32**, 4653 (1985).
 - [11] E. P. Bernard and W. Krauth, *Phys. Rev. Lett.* **107**, 155704 (2011).
 - [12] M. Engel, J. A. Anderson, S. C. Glotzer, M. Isobe, E. P. Bernard, and W. Krauth, *Phys. Rev. E* **87**, 042134 (2013).
 - [13] J. Talbot, G. Tarjus, and P. Viot, *Phys. Rev. E* **61**, 5429 (2000).
 - [14] I. Lončarević, L. Budinski-Petković, and S. Vrhovac, *Phys. Rev. E* **76**, 031104 (2007).

- [15] S. Zarkar, V. Pauchard, U. Farooq, A. Couzis, and S. Banerjee, *Langmuir* **31**, 4878 (2015).
- [16] R. Ghaskadvi and M. Dennin, *Phys. Rev. E* **61**, 1232 (2000).
- [17] D. K. Beaman, E. J. Robertson, and G. L. Richmond, *Proc. Natl. Acad. Sci. U.S.A.* **109**, 3226 (2012).
- [18] S.-Q. Liu, J.-J. Xu, and H.-Y. Chen, *Colloids Surf., B* **36**, 155 (2004).
- [19] V. Fainerman, R. Miller, J. K. Ferri, H. Watzke, M. Leser, and M. Michel, *Adv. Colloid Interface Sci.* **123**, 163 (2006).
- [20] H. Wege, J. Holgado-Terriza, A. Neumann, and M. Cabrerizo-Vilchez, *Colloids Surf. A Physicochem. Eng. Asp.* **156**, 509 (1999).
- [21] V. Fainerman, M. Leser, M. Michel, E. Lucassen-Reynders, and R. Miller, *J. Phys. Chem. B* **109**, 9672 (2005).
- [22] I. Langmuir, *J. Am. Chem. Soc.* **40**, 1361 (1918).
- [23] J. P. Rane, S. Zarkar, V. Pauchard, O. C. Mullins, D. Christie, A. B. Andrews, A. E. Pomerantz, and S. Banerjee, *Energy Fuels* **29**, 3584 (2015).
- [24] J. P. Rane, V. Pauchard, A. Couzis, and S. Banerjee, *Langmuir* **29**, 4750 (2013).
- [25] E. Lucassen-Reynders, *J. Phys. Chem.* **70**, 1777 (1966).
- [26] R. Wuestneck, R. Miller, J. Kriwanek, and H.-R. Holzbauer, *Langmuir* **10**, 3738 (1994).
- [27] V. Fainerman, E. Lucassen-Reynders, and R. Miller, *Colloids Surf. A Physicochem. Eng. Asp.* **143**, 141 (1998).
- [28] P. Joos, *Biochim Biophys Acta Biomembr* **375**, 1 (1975).
- [29] H. C. M. Fernandes, Y. Levin, and J. J. Arenzon, *Phys. Rev. E* **75**, 052101 (2007).
- [30] J. Kundu and R. Rajesh, *Phys. Rev. E* **89**, 052124 (2014).
- [31] F. Sanchez-Varretti, P. Pasinetti, F. Bulnes, and A. Ramirez-Pastor, *Surface Science* **701**, 121698 (2020).
- [32] D. Mandal, T. Nath, and R. Rajesh, *Phys. Rev. E* **97**, 032131 (2018).
- [33] G. A. Iglesias Panuska, P. M. Centres, and A. J. Ramirez-Pastor, *Phys. Rev. E* **102**, 032123 (2020).
- [34] F. C. Thewes and H. C. M. Fernandes, *Phys. Rev. E* **101**, 062138 (2020).
- [35] A. Cadilhe, N. Araújo, and V. Privman, *J. Phys.: Condens. Matter* **19**, 065124 (2007).
- [36] E. Frey and A. Vilfan, *Chem. Phys.* **284**, 287 (2002).
- [37] Z. Adamczyk, *Curr Opin Colloid Interface Sci* **17**, 173 (2012).
- [38] J. J. Ramsden, *J. Phys. Chem.* **96**, 3388 (1992).
- [39] V. Privman, in *Annual Reviews Of Computational Physics III* (World Scientific, 1995) pp. 177–193.
- [40] S. Ji, C. Ates, and I. Lesanovsky, *Phys. Rev. Lett.* **107**, 060406 (2011).
- [41] M. Lackinger, S. Griessl, T. Markert, F. Jamitzky, and W. M. Heckl, *J. Phys. Chem. B* **108**, 13652 (2004).
- [42] Y. Zhang, V. Blum, and K. Reuter, *Phys. Rev. B* **75**, 235406 (2007).
- [43] R. J. Baxter, *Exactly solved models in statistical mechanics* (Elsevier, 2016).
- [44] A. Bellemans and R. Nigam, *J. Chem. Phys.* **46**, 2922 (1967).
- [45] J. Orban and A. Bellemans, *J. Chem. Phys.* **49**, 363 (1968).
- [46] F. H. Ree and D. A. Chesnut, *J. Chem. Phys.* **45**, 3983 (1966).
- [47] L. Runnels, L. Combs, and J. P. Salvant, *J. Chem. Phys.* **47**, 4015 (1967).
- [48] L. Runnels and L. Combs, *J. Chem. Phys.* **45**, 2482 (1966).
- [49] X. Feng, H. W. Blöte, and B. Nienhuis, *Phys. Rev. E* **83**, 061153 (2011).
- [50] Z. Rotman and E. Eisenberg, *Phys. Rev. E* **80**, 031126 (2009).
- [51] D. S. Gaunt and M. E. Fisher, *J. Chem. Phys.* **43**, 2840 (1965).
- [52] D. S. Gaunt, *J. Chem. Phys.* **46**, 3237 (1967).
- [53] E. Eisenberg and A. Baram, *Eur. Phys. Lett.* **71**, 900 (2005).
- [54] M. Ushcats, *Phys. Rev. E* **91**, 052144 (2015).
- [55] M. Ushcats, L. Bulavin, V. Sysoev, and S. Ushcats, *Phys. Rev. E* **94**, 012143 (2016).
- [56] E. Cowley, *J. Chem. Phys.* **71**, 458 (1979).
- [57] D. Burley, *Proc. Phys. Soc.* **75**, 262 (1960).
- [58] H. Hansen-Goos and M. Weigt, *J. Stat. Mech. Theory Exp.* **2005**, P04006 (2005).
- [59] K. Binder and D. Landau, *Phys. Rev. B* **21**, 1941 (1980).
- [60] D. A. Chesnut, *J. Comput. Phys.* **7**, 409 (1971).
- [61] D.-J. Liu and J. W. Evans, *Phys. Rev. B* **62**, 2134 (2000).
- [62] H. C. M. Fernandes, J. J. Arenzon, and Y. Levin, *J. Chem. Phys.* **126**, 114508 (2007).
- [63] T. Nath and R. Rajesh, *Phys. Rev. E* **90**, 012120 (2014).
- [64] G. S. Rushbrooke and H. Scoins, *Proc. Math. Phys. Eng. Sci.* **230**, 74 (1955).
- [65] L. Lafuente and J. A. Cuesta, *Phys. Rev. E* **68**, 066120 (2003).
- [66] S. Darjani, J. Koplik, and V. Pauchard, *Phys. Rev. E* **96**, 052803 (2017).
- [67] S. Darjani, J. Koplik, S. Banerjee, and V. Pauchard, *J. Chem. Phys.* **151**, 104702 (2019).
- [68] J. W. Evans, *Rev. Mod. Phys.* **65**, 1281 (1993).
- [69] M. Nicodemi and A. Coniglio, *Phys. Rev. Lett.* **82**, 916 (1999).
- [70] C. Mak, *Phys. Rev. E* **73**, 065104 (2006).
- [71] K. Wierschem and E. Manousakis, *Phys. Rev. B* **83**, 214108 (2011).
- [72] W. Zhang and Y. Deng, *Phys. Rev. E* **78**, 031103 (2008).
- [73] J.-M. Debierre and L. Turban, *Phys. Lett. A* **97**, 235 (1983).
- [74] R. Baxter, *Ann Comb* **3**, 191 (1999).
- [75] D. Poland, *Phys. Rev. E* **59**, 1523 (1999).
- [76] F. O. Sanchez-Varretti, F. M. Bulnes, and A. J. Ramirez-Pastor, *Adsorption* **25**, 1317 (2019).
- [77] W. J. Ceyrolles, P. Viot, and J. Talbot, *Langmuir* **18**, 1112 (2002).
- [78] X. Jin, J. Talbot, and N.-H. L. Wang, *AIChE J* **40**, 1685 (1994).
- [79] J. Talbot, X. Jin, and N.-H. Wang, *Langmuir* **10**, 1663 (1994).
- [80] G. Tarjus, P. Schaaf, and J. Talbot, *J. Chem. Phys.* **93**, 8352 (1990).
- [81] L. F. Cugliandolo, in *Course 7: dynamics of glassy systems Slow Relaxations and Nonequilibrium Dynamics in Condensed Matter (Les Houches vol 77)* ed J L Barrat, M Feigelman, J Kurchan and J Dalibard (Springer, Berlin, Heidelberg, 2003) pp. 367–521.
- [82] J. Šćepanović, D. Stojiljković, Z. Jakšić, L. Budinski-Petković, and S. Vrhovac, *Physica A* **451**, 213 (2016).
- [83] F. Ritort and P. Sollich, *Adv. Phys.* **52**, 219 (2003).
- [84] A. J. Kolan, E. R. Nowak, and A. V. Tkachenko, *Phys. Rev. E* **59**, 3094 (1999).

- [85] L. F. Cugliandolo, in *Slow Relaxations and nonequilibrium dynamics in condensed matter* (Springer, 2003) pp. 367–521.
- [86] L. F. Cugliandolo and J. Kurchan, Phys. Rev. Lett. **71**, 173 (1993).
- [87] D. Frenkel, Physica A **263**, 26 (1999).
- [88] T. M. Nieuwenhuizen, Phys. Rev. Lett. **80**, 5580 (1998).